Inorg. Chem. **2008**, *47*, 6493−6501

Magnetic and Dielectric Properties of $InFe_2O_4$, $InFeCuO_4$, and $InGaCuO_4$

Kenji Yoshii,*,† Naoshi Ikeda,‡ Yuka Okajima,† Yasuhiro Yoneda,† Yoji Matsuo,§ Yoichi Horibe,|| and Shigeo Mori⊥

Japan Atomic Energy Agency, Sayo, Hyogo 679-5148, Japan, Department of Physics, Okayama University, Okayama 700-8530, Japan, Department of Physics, Osaka Prefecture University, Osaka 599-8531, Japan, Department of Physics and Astronomy, Rutgers, The State University of New Jersey, New Brunswick, New Jersey 08854-8019, and Department of Materials Science, Osaka Prefecture University, Osaka 599-8531, Japan

Received December 5, 2007

The magnetic and dielectric properties of $InFe_2O_4$, $InFeCuO_4$, and $InGaCuO_4$ have been investigated. All these materials are isostructural with RFe_2O_4 (R = Y, Ho−Lu), which shows ferroelectricity due to iron-valence ordering. $InFe_2O_4$ exhibits ferrimagnetic ordering at $T_C \sim 242$ K and a dielectric constant (ε) of ∼10000 at around room temperature. These properties resemble those of RFe_2O_4; the origins of the magnetic and dielectric phenomena are likely common in $InFe_2O_4$ and RFe_2O_4. From measurements of the other two materials, we found that both T_C and ε are decreased in the order of $InFe_2O_4$, $InFeCuO_4$, and $InGaCuO_4$. This result strongly supports the previously reported explanation based on an electron transfer between the Fe-site ions for the corresponding rare-earth systems. Therefore, we propose that the dielectric properties of the oxides isostructural with RFe_2O_4 are plausibly governed by electron transfer; this situation is different from that of ordinary ferroelectrics and dielectrics, in which the displacement of cations and anions is important. In addition, $InFeCuO_4$ and $InGaCuO_4$ exhibit large ε values ($\varepsilon >$ ∼1500). In consideration of this property, we discuss the possible applications of these oxides.

Introduction

Recently, we reported a new mechanism of ferroelectricity in the rare-earth iron oxides RFe_2O_4 (R = Y, Ho−Lu).[1] The system, which has a rhombohedral structure ($R\bar{3}m$),[2,3] shows real-space charge ordering of Fe^{2+} and Fe^{3+} at ∼330 K because of a frustrated charge interaction between the equimolar Fe^{2+} and Fe^{3+} ions on a triangular lattice.[4−10] Because this ordered structure, denoted as the $\sqrt{3} \times \sqrt{3}$ structure, has an electric dipole (Figure 1), a ferroelectric state appears below ∼330 K. This mechanism is apparently different from that of ordinary ferroelectrics, in which the displacement of cations and anions plays a central role.[11]

Both the Fe^{2+} and Fe^{3+} ions in RFe_2O_4 have localized magnetic moments, leading to ferrimagnetic ordering below ∼250 K.[12−16] Thus, these oxides are in a new class of the multiferroic system. A correlation between the magnetic and

* To whom correspondence should be addressed. E-mail: yoshiike@spring8.or.jp. Phone: +81-791-58-2637. Fax: +81-791-58-0311.
† Japan Atomic Energy Agency.
‡ Okayama University.
§ Department of Physics, Osaka Prefecture University.
|| The State University of New Jersey.
⊥ Department of Materials Science, Osaka Prefecture University.

(1) Ikeda, N.; Ohsumi, H.; Ohwada, K.; Ishii, K.; Inami, T.; Murakami, Y.; Kakurai, K.; Yoshii, K.; Mori, S.; Horibe, Y.; Kito, H. *Nature (London)* **2005**, *436*, 1136.
(2) Kimizuka, N.; Takenaka, A.; Sasada, Y.; Katsura, T. *Solid State Commun.* **1974**, *15*, 1321.
(3) Kimizuka, N.; Muromachi, E.; Siratori, K. *Handbook on the Physics and Chemistry of Rare Earths*; Elsevier Science Press: Amsterdam, 1990; Vol. *13*, p 283.
(4) Ikeda, N.; Kohn, K.; Kito, H.; Akimitsu, J.; Siratori, K. *J. Phys. Soc. Jpn.* **1994**, *63*, 4556.
(5) Ikeda, N.; Kohn, K.; Kito, H.; Akimitsu, J.; Siratori, K. *J. Phys. Soc. Jpn.* **1995**, *64*, 1371.
(6) Yamada, Y.; Nohdo, S.; Ikeda, N. *J. Phys. Soc. Jpn.* **1997**, *66*, 3733.
(7) Ikeda, N.; Yamada, Y.; Nohdo, S.; Inami, T.; Katano, S. *Physica B* **1998**, *241−243*, 820.
(8) Ikeda, N.; Kohn, K.; Myouga, N.; Takahashi, E.; Kitoh, H.; Takekawa, S. *J. Phys. Soc. Jpn.* **2000**, *69*, 1526.
(9) Ikeda, N.; Mori, R.; Kohn, K.; Mizumaki, M.; Akao, T. *Ferroelectrics* **2002**, *272*, 309.
(10) Ikeda, N.; Mori, R.; Mori, S.; Kohn, K. *Ferroelectrics* **2003**, *286*, 175.
(11) See, for example, Kittel, C. *Introduction to Solid State Physics*, 8th ed.; Wiley: New York, 2004.
(12) Nakagawa, Y.; Inazumi, M.; Kimizuka, N.; Siratori, K. *J. Phys. Soc. Jpn.* **1979**, *47*, 1369.
(13) Kishi, M.; Miura, S.; Nakagawa, Y.; Kimizuka, N.; Shindo, I.; Siratori, K. *J. Phys. Soc. Jpn.* **1982**, *51*, 2801.
(14) Iida, J.; Tanaka, M.; Kito, H.; Akimitsu, J. *J. Phys. Soc. Jpn.* **1990**, *59*, 4190.
(15) Iida, J.; Tanaka, M.; Nakagawa, Y.; Funahashi, S.; Kimizuka, N.; Takekawa, S. *J. Phys. Soc. Jpn.* **1993**, *62*, 1723.
(16) Yoshii, K.; Ikeda, N.; Nakamura, A. *Physica B* **2006**, *378−380*, 585.

10.1021/ic702365k CCC: $40.75
Published on Web 06/20/2008

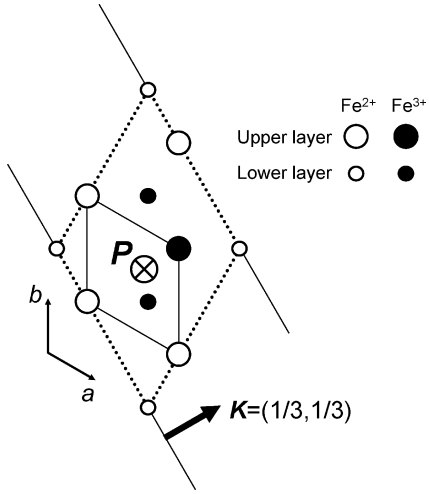

Figure 1. Charge-ordered $\sqrt{3} \times \sqrt{3}$ structure in the *W*-layer of $R\mathrm{Fe_2O_4}$, viewed along the *c*-axis. This structure is accompanied by a charge wave shown by the vector *K*. The *W*-layer consists of the adjacent upper and lower layers of the Fe ions. Dotted lines show the charge-ordered superlattice, inside of which the chemical unit cell is drawn by solid lines. The Fe^{2+} and Fe^{3+} ions are represented by open and filled circles, respectively. Large and small circles stand for the Fe ions in the upper and lower layers, respectively. The 3d electrons in the Fe ions are excessive in the upper layer (Fe^{2+}-rich) but deficient in the lower layer (Fe^{3+}-rich). Thus, an electric polarization (*P*) appears along the *c*-axis. The vector *P* is directed from the upper to the lower layer.

ferroelectric properties is suggested by anomalous electric polarization around ~250 K;[1] the giant magnetodielectic effect at room temperature (ref 17) may indicate that such a correlation exists at lower temperatures.

This system is also interesting in terms of its application. The small activation energy required to flip the direction of each polar region (~0.29 eV) offers the possibility of formulating fatigue-free devices using $R\mathrm{Fe_2O_4}$.[1] The absence of Pb is also suitable for application since lead-free ferroelectrics are desired to reduce environmental burdens.[18]

It is known that Fe ions in $R\mathrm{Fe_2O_4}$ can be replaced by several other cations. The replacement leads to compounds of the form $RM_1M_2\mathrm{O_4}$ ($M_1^{3+} = \mathrm{Fe^{3+}}$ and $\mathrm{Ga^{3+}}$, $M_2^{2+} = \mathrm{Mg^{2+}}$, $\mathrm{Mn^{2+}}$, $\mathrm{Co^{2+}}$, $\mathrm{Cu^{2+}}$ and $\mathrm{Zn^{2+}}$),[19–24] in which the M_1 and M_2 ions are randomly settled at the Fe site in $R\mathrm{Fe_2O_4}$. Although these materials are expected to show interesting physical properties, few studies of the properties have been reported.[21–24] Dielectric phenomena, in particular, have not been studied.

We recently reported the properties of $R\mathrm{Fe_2O_4}$ and its substituted materials (R = Tm, Yb, and Lu).[25–27] A systematic study for R = Yb and Lu showed that the dielectric constant became smaller in the order of $R\mathrm{Fe_2O_4}$, $RF\mathrm{eCoO_4}$, $R\mathrm{FeCuO_4}$, and $R\mathrm{GaCuO_4}$.[27] This phenomenon was explained in connection with a decrease in the electron transfer, as well as the short-range $\sqrt{3} \times \sqrt{3}$ structure of the M_1^{3+} and M_2^{2+} ions (M_1 = Fe and Ga, M_2 = Fe, Co, and Cu). An electric dipole exists in this structure since M_1^{3+} and M_2^{2+} occupy the Fe^{3+} and Fe^{2+} sites, respectively (Figure 1).

The R^{3+} ions can be also replaced by an indium ion (In^{3+}) in both $R\mathrm{Fe_2O_4}$ and its Fe-site-substituted compounds.[28,29] Their synthesis and crystal structures were reported for some oxides such as $\mathrm{InFe_2O_4}$, $\mathrm{InFe}M\mathrm{O_4}$, $\mathrm{InGaCuO_4}$, and $\mathrm{InGaZnO_4}$ (M = Cu and Zn).[28,29] The ionic radius of the In^{3+} ion with the coordination number of 6 is smaller than that of Lu^{3+}.[28,30] Thus the unit-cell volumes of the In oxides become smaller than those of the corresponding Lu oxides.[27–29]

In this study, we investigated the magnetic and dielectric properties of $\mathrm{InFe_2O_4}$, $\mathrm{InFeCuO_4}$, and $\mathrm{InGaCuO_4}$. The Co-substituted $\mathrm{InFeCoO_4}$ was not studied because of its spinel structure.[28,31] Except for $\mathrm{InFe_2O_4}$, the properties of these materials have not been reported.[32] Whereas $\mathrm{InFe_2O_4}$ has been prepared by a solid-state reaction in an evacuated platinum or silica tube,[29,32] we synthesized this material using essentially the same method as that used for $\mathrm{TmFe_2O_4}$, $\mathrm{YbFe_2O_4}$, and $\mathrm{LuFe_2O_4}$,[16,27] that is, a solid-state reaction in a $\mathrm{CO-CO_2}$ flow. For the purpose of a comparison with the rare-earth systems,[27] the present work deals mainly with the physical properties below 300 K.

Experimental Procedures

All the samples were in a polycrystalline form and were prepared by a solid-state reaction. For the preparation of $\mathrm{InFe_2O_4}$, the starting materials of $\mathrm{In_2O_3}$ (Soekawa, ~99.99%) and $\mathrm{Fe_2O_3}$ (High Purity Chem. Laboratory., ~99.999%) were fired at ~1000 °C for ~48−72 h in air. Then, the mixtures were ground and fired again at ~1000 °C for ~48−72 h in a $\mathrm{CO-CO_2}$ mixed gas. The ratio of the flows of CO and CO_2 was ~25:75 cc/min. After the firing, the samples were quenched to room temperature.[28,29] The weight loss during the firing was almost the same as that expected in the reduction from Fe^{3+} to $Fe^{2.5+}$. From magnetic measurements, an impurity was observed if the firing in air was neglected; the impurity showed a deviation of the field-cooled (FC) and zero-field-cooled (ZFC) magnetic susceptibilities at higher temperatures than the magnetic transition temperature (~240 K). From a weight gain in thermogravimetry up to 1000 °C (Rigaku TAS200), the oxygen content in $\mathrm{InFe_2O_}x$ was estimated to be $x \sim 3.93-3.96(2)$. These values are slightly smaller than those for $R\mathrm{Fe_2O_}x$, $x \sim 3.98(2)$.[27]

The samples of $\mathrm{InFeCuO_4}$ and $\mathrm{InGaCuO_4}$ were prepared by firing in air as was the case for $R\mathrm{FeCuO_4}$ and $R\mathrm{GaCuO_4}$ (R = Yb and Lu).[27] Because CuO is reduced to Cu_2O above 1050 °C, the firing

(17) Subramanian, M. A.; He, T.; Chen, J.; Rogado, N. S.; Calvarese, T. G.; Sleight, A. W. *Adv. Mater. (Weinheim, Ger.)* **2006**, *18*, 1737.
(18) See, for example, Ryu, J.; Choi, J.-J.; Hahn, B.-D.; Park, D.-S.; Yoon, W.-H.; Kim, K.-H. *Appl. Phys. Lett.* **2007**, *90*, 152901.
(19) Kimizuka, N.; Takayama, E. *J. Solid State Chem.* **1981**, *40*, 109.
(20) Kimizuka, N.; Takayama, E. *J. Solid State Chem.* **1982**, *41*, 166.
(21) Iida, J.; Tanaka, M.; Nakagawa, Y. *J. Phys. Soc. Jpn.* **1990**, *59*, 4443.
(22) Sunaga, T.; Tanaka, M.; Sakai, N.; Tsunoda, Y. *J. Phys. Soc. Jpn.* **2001**, *70*, 3713.
(23) Ikeda, N.; Kohn, K.; Himoto, E.; Tanaka, M. *J. Phys. Soc. Jpn.* **1995**, *64*, 4371.
(24) Todate, Y.; Himoto, E.; Kikuta, C.; Tanaka, M.; Suzuki, J. *Phys. Rev.* **1998**, *B57*, 485.
(25) Matsuo, Y.; Horibe, Y.; Mori, S.; Yoshii, K.; Ikeda, N. *J. Magn. Magn. Mater.* **2007**, *310*, 349(E)
(26) Yoshii, K.; Ikeda, N.; Mori, S. *J. Magn. Magn. Mater.* **2007**, *310*, 1154.
(27) Yoshii, K.; Ikeda, N.; Matsuo, Y.; Horibe, Y.; Mori, S. *Phys. Rev.* **2007**, *B76*, 024423.
(28) Kimizuka, N.; Takayama, E. *J. Solid State Chem.* **1984**, *53*, 217.
(29) Kimizuka, N.; Mohri, T. *J. Solid State Chem.* **1985**, *60*, 382.
(30) Shannon, R. D. *Acta Crystallogr., Sect. A: Found. Crystallogr.* **1976**, *A32*, 751.
(31) Sakai, Y.; Kimizuka, N.; Mohri, T.; Tsuda, N. *J. Phys. Soc. Jpn.* **1986**, *55*, 1402.
(32) Oka, K.; Azuma, M.; Narumi, Y.; Koichi, K.; Hayashi, N.; Shimakawa, Y.; Takano, M. *J. Jpn. Soc. Powder Powder Metall.* **2007**, *54*, 53.

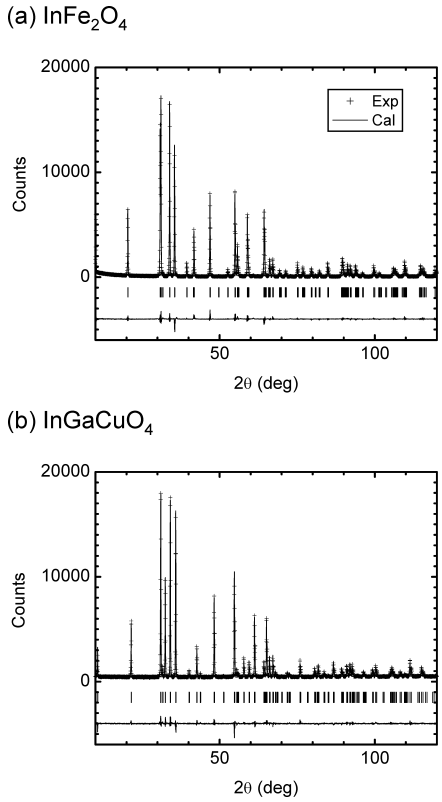

Figure 2. Powder XRD patterns for $InFe_2O_4$ ($R_{WP} \sim 9.13\%$) and $InGaCuO_4$ ($R_{WP} \sim 5.85\%$) fitted with the space group $R\bar{3}m$. The cross markers and upper solid lines stand for the experimental (Exp) and calculated (Cal) patterns, respectively. The lower solid lines show the differences between the experimental and calculated patterns. The vertical markers are the calculated Bragg angles.

temperature was ~1000 °C.[19,33] The starting materials were In_2O_3, Fe_2O_3, CuO, and Ga_2O_3 (Soekawa or High Purity Chem. Laboratory., ~99.99−99.999%). The firing was done for ~3 days to ~1 week and was repeated twice; the weight loss was negligible during these periods. All the samples were quenched after the firing.[28,29] The oxygen content in $InMCuO_x$ (M = Fe and Ga) was larger than $x \sim 3.96(2)$ from thermogravimetry.

The crystal structures were determined by powder X-ray diffraction (XRD) using Cu Kα radiation. The XRD patterns were fitted by the Rietveld method (RIETAN-2000).[34] To observe the valence of the In ions, X-ray absorption measurements were performed using synchrotron radiation at BL14B1 of SPring-8. Photoabsorption of the samples was measured at room temperature while the photon energy was swept around the In-K absorption edge.

The magnetic measurements were carried out with a superconducting quantum interference device (SQUID) magnetometer (Quantum Design MPMS). The dielectric measurements were performed with an LCR meter (HP-4284A) below 300 K while the samples were heated after being cooled down to ~20 K. The other details have been noted elsewhere.[4,5,8,16,27]

Results

(A) XRD and X-ray Absorption. Figure 2 shows the XRD patterns of $InFe_2O_4$ and $InGaCuO_4$. The experimental patterns could be fitted with the $R\bar{3}m$ structure.[28,29,35] The lattice parameters shown in Table 1 are close to those reported in the literature.[28,29] A change of the cell volume by Fe-site substitution is understandable assuming that the radius of Fe^{2+} with the coordination number (CN) of 5 is the average of radii with CNs of 4 and 6.[27,30]

Table 1. Lattice Lengths (a and c) and Unit-Cell Volume (V) for All Three Oxides

Material	a (Å)	c (Å)	V (Å^3)
$InFe_2O_4$	3.3389(1)	26.0609(4)	251.604(8)
$InFeCuO_4$	3.3723(1)	24.8560(5)	244.797(11)
$InGaCuO_4$	3.3514(1)	24.8087(4)	241.318(8)

Figure 3 shows the X-ray absorption near-edge structure (XANES) spectra of $InFe_2O_4$ and $InGaCuO_4$, as well as reference materials (In metal, In_2O_3 and $InGaZnO_4$). On the basis of the selection rule, the photoabsorption corresponds to a transition from In-1s to In-p states. The spectral profiles of $InFe_2O_4$ and $InGaCuO_4$ are similar to that of In_2O_3. Thus, the valences of the In ions are close to 3+. The main absorption peaks (~27.399 keV; middle arrow) are located at a slightly lower energy than that of In_2O_3 (right dotted line with an arrow; ~27.941 keV), perhaps because of the difference in oxygen coordination between the RFe_2O_4-type oxides ($R\bar{3}m$, octahedral coordination) and In_2O_3[36] ($Ia3$, CaF_2-type coordination with periodic vacancies of oxygen).[37]

By using the isostructural $InGaZnO_4$ prepared in air as a reference material,[37] the valences of the In ions in the samples are ~3+. $InGaZnO_4$ becomes conductive by reduction (e.g., firing in an Ar flow)[37] because of electron doping in the In-5s band.[38] Because the present $InGaZnO_4$ was prepared in air, the reduction of the In ion would seem difficult, the carrier density being very low because of the white sample color.

The spectra of all the samples resembled that of $InGaZnO_4$. The positions of the largest absorption peaks (~27.399 keV) were also identical to each other (middle arrow in Figure 3). Thus, the indium valences of $InFe_2O_4$, $InFeCuO_4$, and $InGaCuO_4$ were ~3+, which is reasonable for $InFeCuO_4$ and $InGaCuO_4$ prepared in air. Figure 3 also shows that the In ions in $InFe_2O_4$ maintain the ~3+ state during firing in the reducing atmosphere. This result seems to be in accord with its magnetic transition temperature close to those of RFe_2O_4 (R = Y, Tm, Yb, and Lu) shown just later.

(B) Magnetic Properties. Figure 4a−c shows the direct current (DC) magnetic susceptibility (M/H) plotted against the temperature for $InFe_2O_4$, $InFeCuO_4$, and $InGaCuO_4$, respectively. Some representative parameters are listed in Table 2.

As shown in Figure 4a, the field-cooled (FC) and zero-field-cooled (ZFC) curves of $InFe_2O_4$ are comparable to those reported recently.[32] The susceptibility values stand between those of the magnetically aligned c-axis-parallel and per-

(33) Gadalla, A. M. M.; Ford, W. F.; White, J. *Trans. Brit. Ceram. Soc.* **1963**, *62*, 57.
(34) Izumi, F.; Ikeda, T. *Mater. Sci. Forum* **2000**, *321−324*, 198.
(35) Nespolo, M.; Isobe, M.; Iida, J.; Kimizuka, N. *J. Alloys Compd.* **2000**, *313*, 59.
(36) Marezio, M. *Acta Crystallogr.* **1966**, *20*, 723.
(37) Orita, M.; Takeuchi, M.; Sakai, H.; Tanji, H. *Jpn. J. Appl. Phys.* **1995**, *34*, L1550.
(38) Orita, M.; Tanji, H.; Mizuno, M.; Adachi, H.; Tanaka, I. *Phys. Rev.* **2000**, *B61*, 1811.

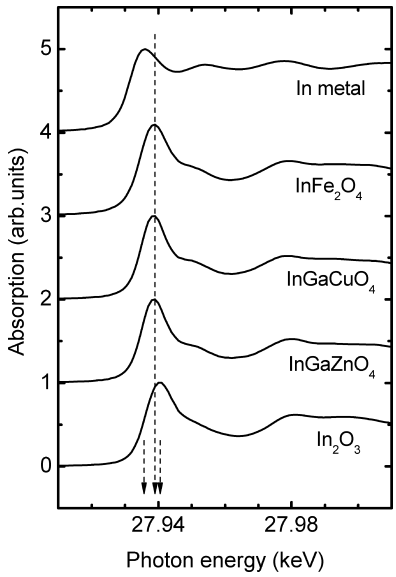

Figure 3. X-ray absorption near-edge structure (XANES) spectra for $InFe_2O_4$ and $InGaCuO_4$ and the reference materials (In metal, $InGaZnO_4$, and In_2O_3) around the In−K edge. The left and right dotted lines accompanied by arrows stand for the energies of the absorption peaks of In metal and In_2O_3, respectively. The middle arrow indicates the peak energies of the samples ($InFe_2O_4$, $InFeCuO_4$, and $InGaCuO_4$), as well as the reference material ($InGaZnO_4$).

pendicular polycrystals.[32] Small peaks of susceptibility are observed at ∼230 K, slightly lower than in the reference (240 K).[32] This behavior may be related to the difference in oxygen content.[4] The thermoremanent magnetization (TRM) shows a magnetic transition temperature of ∼242 K (an arrow), which is nearly the same as that in the reference (240 K).[32] The transition temperature will be tentatively denoted as T_C, as the magnetic structure could not be specified. T_C∼242 K is close to those of RFe_2O_4 (T_C ∼ 240−250 K, R = Y, Tm, Yb, and Lu).[12–16,27] The sample in ref 32 was purified using a magnet to remove the impurity of Fe_3O_4 (Néel temperature of ∼851 K, ref 39). The purification was not carried out because no anomalous behavior was observed; both the FC and ZFC curves traced each other up to 400 K.

The magnetic ordering is induced by Fe^{2+} ($3d^6$; S = 2; 4.90 μ_B) and Fe^{3+} ($3d^5$; S = 5/2; 5.92 μ_B) from the nonmagnetic state of In^{3+}. The existence of TRM suggests ferrimagnetic ordering, as in RFe_2O_4.[12–15] The inverse susceptibility (inset) shows a hyperbolic ferrimagnetic shape.[40] The paramagnetic moment (P_{eff}) from the Curie−Weiss fit was close to that based on the spin-only $Fe^{2+}$and Fe^{3+} moments. The slightly larger P_{eff} value (∼110%) than the estimated value may be attributable to the formation of small magnetic regions, as suggested for $LuFeCuO_4$, in which short-range ionic ordering of Fe^{3+} and Cu^{2+} was observed.[25,27] The Weiss temperature (θ) of ∼ −560 K shows that antiferromagnetic interactions are dominant.

Figure 4b shows that the magnetic transition of $InFeCuO_4$ appears at ∼70 K. Ferrimagnetism is suggested by the

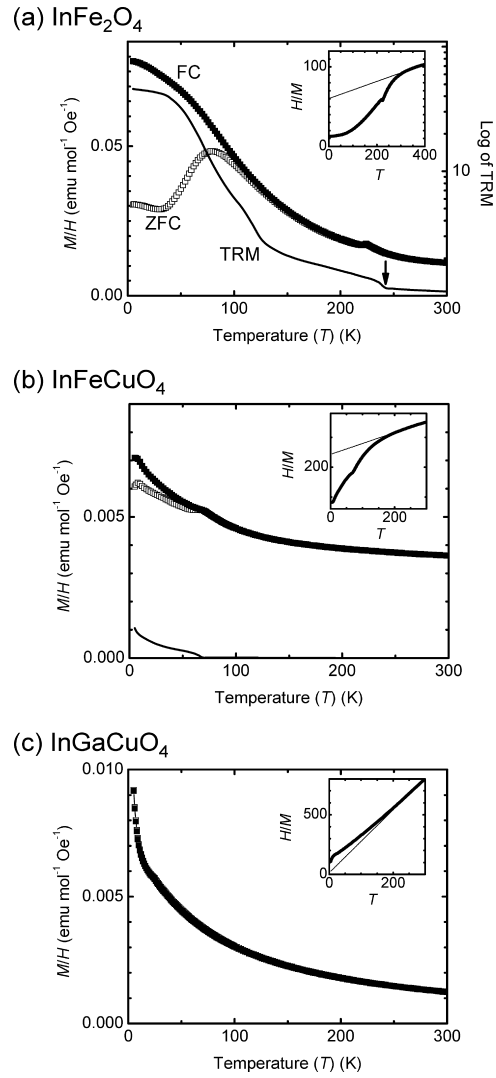

Figure 4. DC magnetic susceptibility (M/H) plotted against the temperature (T) for (a) $InFe_2O_4$, (b) $InFeCuO_4$, and (c) $InGaCuO_4$ (M: magnetization, H: applied magnetic field of 1000 Oe). The filled and open squares are field-cooled (FC) and zero-field-cooled (ZFC) susceptibilities, respectively. The solid lines stand for thermoremanent magnetization (TRM). In (a), TRM is shown in a log scale to emphasize the magnetic transition at 242 K (an allowance). In (b), TRM was divided by 1000 to scale with the susceptibilities. The insets show the inverse susceptibility (thick solid lines) and the Curie−Weiss fit (thin solid lines).

observation of TRM. P_{eff} is ∼6.6 μ_B/formula unit. As found for $InFe_2O_4$ and $LuFeCuO_4$, this is slightly larger than the estimated value (6.2 μ_B/formula unit), assuming the spin-only moments of Fe^{3+} and Cu^{2+} ($3d^1$; S = 1/2; 1.73 μ_B). θ was calculated as ∼ −1200 K. The magnetic transition temperature of ∼70 K is larger than that of $LuFeCuO_4$ (∼47 K), in which Lu^{3+} is nonmagnetic, although similar P_{eff} and θ values were obtained for $LuFeCuO_4$ (P_{eff} = 7.0 μ_B/formula unit and θ = −1300 K).[27] The transition temperature will be denoted as T_C for simplicity (Table 2).

The data for $InGaCuO_4$ are shown in Figure 4c. Very similar FC and ZFC curves, together with the absence of TRM, indicate a lack of magnetic ordering. The Curie−Weiss fit was accomplished by using the spin-only Cu^{2+} moment at a Weiss temperature of almost zero. The Ga ion was in the nonmagnetic 3+ state ($3d^{10}$). The curve deviates from the linear relationship below ∼200 K, possibly because of

(39) See, for example, Bimbi, M.; Allodi, G.; De Renzi, R.; Mazzoli, G.; Berger, H.; Amato, A. *Physica* **2006**, *B374−375*, 45.
(40) Sugihara, T.; Siratori, K.; Shindo, I.; Katsura, T. *J. Phys. Soc. Jpn.* **1978**, *45*, 1191.

Table 2. Representative Parameters Obtained for All the Oxides[a]

material	T_C (K)	θ (K)	P_{eff} (μ_B)	ε (RT)	α	Q (eV)	ρ (ohm cm; RT), E(eV)
$InFe_2O_4$	242	−560	8.6	11000 (300 Hz)	0.15 (130 K)	0.13	$\sim 1-3 \times 10^2$, ∼0.10
$InFeCuO_4$	70	−1200	6.6	6000 (20 Hz)	0.12 (200 K)	0.29	$\sim 2-4 \times 10^6$, ∼0.26
$InGaCuO_4$	none	∼0	1.6	1600 (20 Hz)	0.13 (250 K)	0.41	$\sim 6-9 \times 10^7$, ∼0.44

[a] T_C, magnetic transition temperature (K); θ, Weiss temperature (K); P_{eff}, effective paramagnetic moment (μ_B/unit formula). ε(RT): dielectric constant at room temperature (RT) with the AC field at the lowest frequency of 20 Hz. Only for $InFe_2O_4$ is the value shown at 300 Hz because of the fluctuation of the dielectric constant at frequencies lower than 300 Hz. α, parameter obtained from the Debye fitting for dielectric dispersion. Q, activation energy calculated from tan δ (eV). ρ, AC electrical resistivity at around room temperature extracted from the imaginary part of the dielectric response with the AC fields of ∼20 Hz and ∼0.01−0.1 V/cm (Ω cm). E: activation energy (eV) obtained from the AC resistivity at low frequency (∼20 Hz) at temperatures between ∼80 and ∼300 K, where the peak of tan δ was observed, i.e., where the motion of the polar regions takes place. See the text for details.

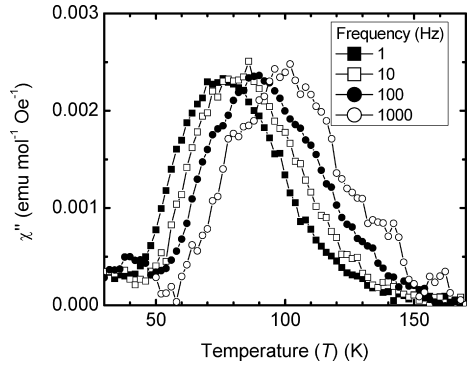

Figure 5. Imaginary part of AC susceptibility (χ'') plotted against the temperature (T) for $InFe_2O_4$. The frequencies of the AC field are also shown.

the development of a coherent arrangement of magnetic moments.

Isothermal magnetization measurements of $InFe_2O_4$ and $InFeCuO_4$ showed small magnetic hysteresis without saturated magnetization, which is consistent with the possible existence of ferrimagnetism. The residual magnetization was less than $\sim 10^{-3}$ emu/formula unit. Magnetic hysteresis was not observed for $InGaCuO_4$.

AC magnetic susceptibility was also measured. For $InFeCuO_4$, the real part exhibited a peak at $T_C \sim 70$ K. The peak shifted slightly with the changing frequency of the AC magnetic field. The temperature shift defined as $(\Delta T/T)/\Delta \log f$ was ∼0.007 (ΔT, difference in the peak temperature; T, peak temperature; $\Delta \log f$, difference in the logarithm of the AC frequency).[41] This result may indicate that the low-temperature magnetic state is attributed to a spin glass rather than to ferrimagnetism.[41] Note also that the magnetic ordering in $InFe_2O_4$ becomes short-ranged by the Fe-site substitution, as it does in the rare-earth systems.[27]

Figure 5 shows the imaginary part of AC magnetic susceptibility for $InFe_2O_4$. A broad peak at ∼100 K exhibits a frequency dependence, which was fitted with the Arrhenius law:[27,42]

$$f = f_0 \exp(-U/kT) \quad (1)$$

Here, f and f_0 are the frequency of the AC field and the preexponential factor, respectively. U, k, and T are the activation energy, Boltzmann constant, and peak temperature, respectively. U corresponds to the energy required to change the direction of magnetization of each magnetic cluster. The calculated U was ∼0.18 eV, which was smaller than that of $LuFe_2O_4$ ($U \sim 0.28-0.3$ eV).[27,42] Although we have no explanation for this difference, it is noteworthy that this U is close to the activation energy obtained from the dielectric response shown later (Q; ∼0.13 eV). This result implies a correlation between the magnetic and dielectric properties (i.e., multiferroicity), as in $LuFe_2O_4$.[27] For $InFeCuO_4$, U could not be determined because of the very small values of the imaginary part (less than 10^{-5} emu mol $^{-1}$ Oe^{-1}).

(C) Dielectric Properties. Figure 6a shows the temperature dependence of the dielectric constant (ε) for $InFe_2O_4$. At a glance, ε exhibits large values of ∼10000 at around room temperature (Table 2), as reported for RFe_2O_4 (R = Er, Tm, Yb, and Lu, $\varepsilon \sim 5000-30000$).[1,4,5,8,16,26,27] The largest ε of $InFe_2O_4$ reported previously was ∼8.[32] In this reference, a small peak of ε was observed at around T_C (∼240 K). However, such a phenomenon is not shown in Figure 6a. Although the reason for these differences is unclear, the present data appear to be relevant since the temperature dependencies of ε provide shapes analogous to those of RFe_2O_4.[1,4,5,8,16,26,27] Together with the large ε, the results strongly suggest that the polar regions originate from a charge-ordered state such as that in RFe_2O_4.[1] Figure 6a also shows that ε is changed by the AC frequency, a behavior known as dielectric dispersion, which will be discussed later.

The loss term (tan δ) was found to exhibit a peak below 180 K, lower than that of RFe_2O_4 (R = Er, Tm, Yb, and Lu); the peak appeared below 230−250 K in these oxides.[1,4,5,8,16] As a peak of tan δ corresponds to a relaxation of electric dipoles,[1,4,8,43] the motion of the polar regions in $InFe_2O_4$ occurs at temperatures lower than those of RFe_2O_4. The peak temperature and frequency of the AC electric field were fitted with the same type of formula as Eq. 1:

$$f = f_0 \exp(-Q/kT) \quad (2)$$

Here, f and f_0 are the frequency of the AC field and the preexponential factor, respectively. Q, k, and T are the activation energy, Boltzmann constant, and peak temperature, respectively. Q can be regarded as the energy required for the reorientation of each polar region.[1,4,43] The calculated Q of ∼0.13 eV in Table 2 is close to U and is smaller than those of RFe_2O_4 and $Q \sim 0.26-0.30$ eV.[1,4,5,8,16,27] The latter result means that the polar regions are more easily rotated by a lower thermal activation in $InFe_2O_4$ than in RFe_2O_4,

(41) Mydosh, J. A. *Spin Glasses*; Taylor and Francis: London, 1993.
(42) Ikeda, N.; Kohn, K.; Siratori, K.; Iida, J.; Tanaka, M.; Nakagawa, Y.; Kimizuka, N.; Takekawa, S. *Ferrites: Proceedings of the 6th International Conference on Ferrites (ICF6)*; Japan Society of Powder and Powder Metallurgy: Kyoto, 1992; p 711.
(43) Zipse, D.; Dalal, N. S.; Vasic, R.; Brooks, J. S.; Kögerler, P. *Phys. Rev.* **2005**, *B71*, 064417.

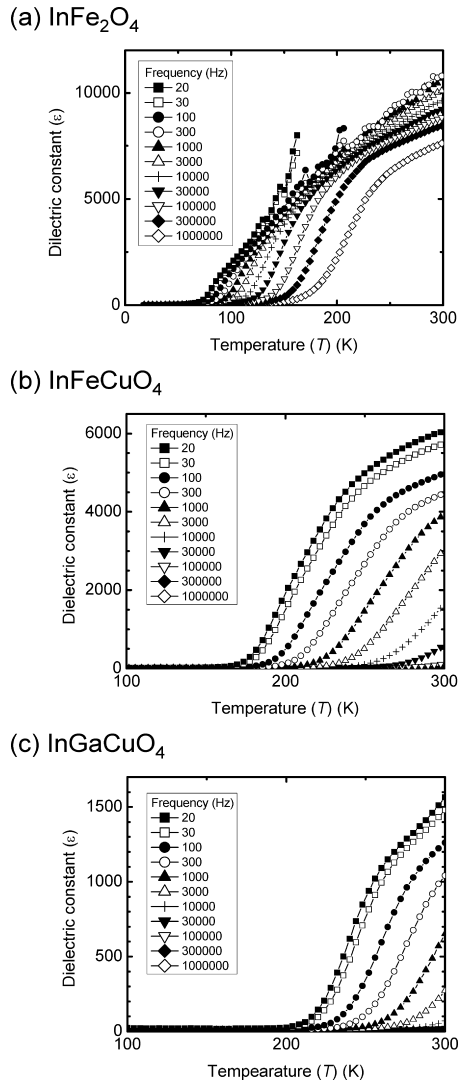

Figure 6. Dielectric constant (ε) plotted against the temperature (T) for (a) $InFe_2O_4$, (b) $InFeCuO_4$, and (c) $InGaCuO_4$. The frequencies of the AC electric field are also shown.

consistent with the observed peak temperatures of tan δ for $InFe_2O_4$and RFe_2O_4.

Figure 6b,c shows the dielectric constant (ε) for $InFeCuO_4$ and $InGaCuO_4$, respectively. The ε values of $InFeCuO_4$ and $InGaCuO_4$ in the low frequencies ($\sim$20$-$30 Hz) are $\sim$6000 and $\sim$1600, respectively (Table 2). These are considerably larger than those of corresponding rare-earth oxides; the ε values of $RFeCuO_4$ and $RGaCuO_4$ were $\sim$100$-$200 and $\sim$10, respectively (R = Yb and Lu).[27]

The dielectric dispersion was fitted with the so-called Debye model:[4,27]

$$\varepsilon = \varepsilon_1/(1 + (i\tau\omega)^{1-\alpha}) + \varepsilon_2 \quad (3)$$

Here, τ is the center of the fluctuation time of each polar region while ω is the angular frequency ($\omega = 2\pi f$). The parameter of α reflects the distribution width of the fluctuation time of each polar region.[4] Therefore, if this value is small (i.e., $\alpha \sim 0$), the response of the polar regions is coherent. Figure 7a shows the dielectric dispersion below $\sim$250 K. For $InFe_2O_4$, a meaningful fitting was obtained only below $\sim$130 K because a change in ε was not very apparent

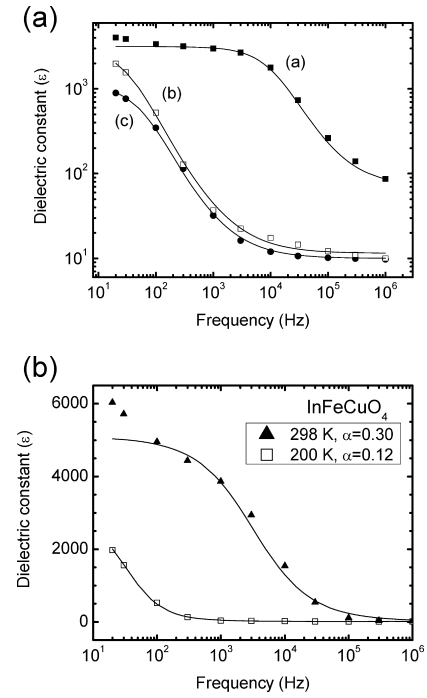

Figure 7. (a) Dielectric dispersion for (a) $InFe_2O_4$ (130 K, $\alpha\sim$0.15), (b) $InFeCuO_4$ (200 K, $\alpha\sim$0.12), and (c) $InGaCuO_4$ (250 K, $\alpha\sim$0.13). (b) Dielectric dispersion of $InFeCuO_4$ at 200 and 298 K. The experimental data are shown by the markers while the fitted data are drawn with the solid lines.

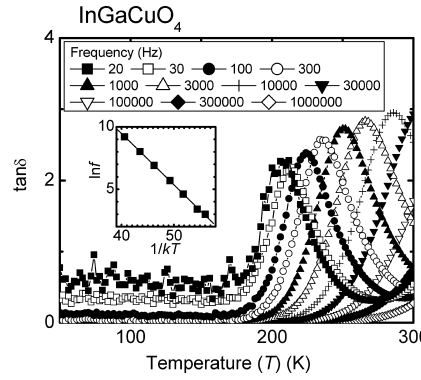

Figure 8. tan δ plotted against the temperature (T) for $InGaCuO_4$. The frequencies of the AC electric field are shown as well. The inset shows the Arrhenius fitting (solid line) for the peak temperature of tan δ (filled squares). The ordinate scale stands for the natural logarithm of the AC frequency while the abscissa is $1/kT$ in terms of eV (k, Boltzmann constant; T, peak temperature).

above $\sim$130 K. The parameter α was calculated as $\sim$0.15 (Table 2), which was larger than those of RFe_2O_4 ($\alpha \sim 0.1$, R = Er, Yb, and Lu);[4,5,27] accordingly, a coherency was suppressed in $InFe_2O_4$. For the other materials, the α values were $\sim$0.12$-$0.15 below $\sim$250 K (Table 2). As demonstrated in Figure 7b, α was increased by increasing the temperature for $InFeCuO_4$ and $InGaCuO_4$. At $\sim$ 300 K, α was calculated as $\sim$0.30, comparable to the values for $RFeCoO_4$, $RFeCuO_4$, and $RGaCuO_4$ at $\sim$300 K ($\alpha \sim 0.3-0.4$, R = Yb and Lu).[27]

In Figure 8, a peak of tan δ is shown for $InGaCuO_4$. This peak could not be detected for $RFeCuO_4$ and $RGaCuO_4$ below 300 K (R = Yb and Lu).[27] The experimental data and the fitting by eq 2 are shown in the inset. The calculated Q values of $InFeCuO_4$ and $InGaCuO_4$ are $\sim$0.29 and $\sim$0.41 eV, respectively. The Q of $InFeCuO_4$ is nearly identical to

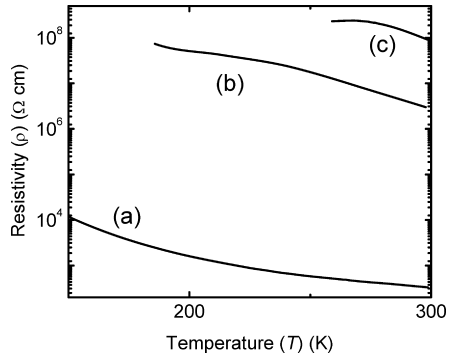

Figure 9. AC electrical resistivity (ρ) plotted against the temperature (T) for (a) $InFe_2O_4$, (b) $InFeCuO_4$, and (c) $InGaCuO_4$, with an AC frequency of 20 Hz.

those of RFe_2O_4 ($Q \sim 0.26$–0.30 eV).[1,4,5,8,16,27] On the other hand, the value of $InGaCuO_4$ ($Q \sim 0.41$ eV) is close to that of $RFeCoO_4$ ($Q \sim 0.37$ eV, R = Yb and Lu).[27] The obtained parameters are listed in Table 2.

Discussion

The overall physical properties of the present materials (Table 2) seem to resemble those of the corresponding Yb and Lu oxides,[27] which is reasonable because the ionic radii of Yb^{3+}, Lu^{3+}, and In^{3+} are comparable to each other.[30] The Q values (Table 2) are smaller than those of ordinary ferroelectrics and dielectrics, for example, $Q \sim 0.9$ eV for $Pb(Zr_{0.2}Ti_{0.8})O_3$ (PZT) films,[44] suggesting that the dielectric properties are rooted not in the ordinary mechanism (i.e., displacement of cations and anions) but in the transfer of electrons as in RFe_2O_4,[1] as the Q values are rather close to those of RFe_2O_4. In addition, both T_C and ε are decreased in the order of $InFe_2O_4$, $InFeCuO_4$, and $InGaCuO_4$. The ε values of $InFeCuO_4$ and $InGaCuO_4$ are considerably larger than those of the Yb- and Lu oxides.

Below, a discussion of these phenomena is given by comparing indium oxides with each other and with the rare-earth series. A brief comment on possible applications is made as well. For convenience, the label of R will stand for the rare-earth elements of Yb and Lu, except as otherwise specified.

(A) Comparison of $InFe_2O_4$, $InFeCuO_4$, and $InGaCuO_4$. In previous studies, AC resistivity was derived from the imaginary part of the dielectric response.[27,45] The data at the lowest AC frequency (20 Hz) at around room temperature are shown in Figure 9. The resistivity (ρ) at around room temperature is given in Table 2.

The figure shows that all the materials are either semiconducting or insulating. The 3+ valence of the In ions (Figure 3) indicates that the conduction is mainly due to the 3d bands of the Fe-site ions.[38] The resistivity of $\rho \sim 100$ Ω cm of $InFe_2O_4$ appears to be smaller than that of RFe_2O_4 ($\rho \sim 100-1000$ Ω cm),[27] possibly related to the different oxygen contents shown in the Experimental Procedures.[4] Note also that the resistivity inside the a-b plane in RFe_2O_4 is much smaller ($\sim$1/10) than that along the c-axis.[46] Therefore, the shrinkage of the a-length (Table 1) may have a dominant effect on the decrease in resistivity. This shrinkage seems to be associated with $InFeCuO_4$ and $InGaCuO_4$, which show smaller resistivity than do $RFeCuO_4$ ($\rho \sim 10^8$ Ω cm) and $RGaCuO_4$ ($\rho > \sim 10^8-10^9$ Ω cm), respectively.[27]

The resistivity is increased in the order of $InFe_2O_4$, $InFeCuO_4$, and $InGaCuO_4$. The larger resistivity of $InFeCuO_4$ than that of $InFe_2O_4$ (Figure 9, Table 2) is explained in terms of the weakening of hybridization between the 3d orbitals of the neighboring Fe-site ions.[27] The highest resistivity of $InGaCuO_4$ is attributable to the existence of the closed-shell Ga^{3+} ion.

It seems likely that the differences in T_C in $InFe_2O_4$, $InFeCuO_4$, and $InGaCuO_4$ are related to the spin value of the magnetic ion as well as the exchange interaction.[27,47] The spin values of the Fe-site ions are in accord with T_C, considering the spin-only moments of Fe^{3+} (5.92 μ_B), Fe^{2+} (4.90 μ_B), Cu^{2+} (1.73 μ_B), and Ga^{3+} (0 μ_B). The change of T_C is also understandable in connection with the exchange interaction (J), which is given by $J \sim t^2/U$ (t; electron transfer, U; Coulomb repulsion).[47] The electron transfer manifests itself as the electrical resistivity (Figure 9), which indicates a decrease in exchange interaction in the order of $InFe_2O_4$, $InFeCuO_4$, and $InGaCuO_4$. The absolute value of θ of $InFeCuO_4$ (1200 K, Table 2), which is affected by J, are not consistent with the change of T_C. This result shows the possible importance of the magnetic frustration on a triangular lattice, which may be also true for $LuFeCuO_4$.[27] To obtain further information, magnetic measurements at higher temperatures are necessary.

Small magnetic regions were found in $InFeCuO_4$ from the real part of the AC magnetic susceptibility, as noted earlier. Such regions are created by the magnetic dilution, as shown for $LuFeMgO_4$,[23] in which strong Fe−Fe magnetic interactions are weakened by the nonmagnetic Mg^{2+} ion. The dilution gives rise to the distribution and shrinkage of the magnetic clusters[23] and leads to a resistivity lower than that of $InFe_2O_4$ (Figure 9).

The change of the dielectric constant (ε) for the rare-earth series was interpreted as follows.[27] The dielectric response in RFe_2O_4 is due to the polar $\sqrt{3} \times \sqrt{3}$ structure (Figure 1).[1] Similar ionic ordering of M_1^{3+} and M_2^{2+} with a short-range $\sqrt{3} \times \sqrt{3}$ structure is expected for $RM_1M_2O_4$ (M_1 = Fe and Ga, M_2 = Co and Cu) from the electron-microscopic measurement of $LuFeCuO_4$.[25] This structure has an electric dipole, with M_1^{3+} settled at the Fe^{3+} site and M_2^{2+} at the Fe^{2+} site (Figure 1). For RFe_2O_4, the large dielectric constants are rooted in a reversal of the polar regions arising from the electron transfer between Fe^{3+} and Fe^{2+}.[1] The AC resistivity showed that the electron transfer was suppressed in the order

(44) Ganpule, C. S.; Roytburd, A. L.; Nagarajan, V.; Hill, B. K.; Ogale, S. B.; Williams, E. D.; Ramesh, R.; Scott, J. F. *Phys. Rev.* **2001**, *B65*, 014101.
(45) Mazzara, G. P.; Skirius, S.; Cao, G.; Chern, G.; Clark, R. J.; Crow, J. E.; Mathias, H.; O'Reilly, J. W.; Testardi, L. R. *Phys. Rev.* **1993**, *B47*, 8119.
(46) Tanaka, M.; Akimitsu, J.; Inada, Y.; Kimizuka, N.; Shindo, I.; Siratori, K. *Solid State Commun.* **1982**, *44*, 687.
(47) See, for example, Yosida, K. *Theory of Magnetism*; Springer: New York, 1996.

of RFe$_2$O$_4$, RFeCoO$_4$, RFeCuO$_4$, and RGaCuO$_4$. Thus, the response of the polar regions becomes more difficult in this order, and ε exhibits the following tendency: $\varepsilon(R\text{Fe}_2\text{O}_4) > \varepsilon(R\text{FeCoO}_4) > \varepsilon(R\text{FeCuO}_4) > \varepsilon(R\text{GaCuO}_4)$.

This explanation is probably applicable for InFe$_2$O$_4$, InFeCuO$_4$, and InGaCuO$_4$, based on the results shown in Table 2 and in Figures 6 and 9. The similar values of Q and E (activation energy obtained from the resistivity, Table 2) strongly suggest the importance of electron transfer, which is also supported by the small Q values. Interestingly, the values of Q close to E may indicate that the directions of the polar regions are changed by the electron transfer, giving rise to the dielectric response. Namely, the electric dipole in the $\sqrt{3} \times \sqrt{3}$ ionic ordering of M_1^{3+} and M_2^{2+} flips its direction if the ionic configuration of $M_1^{3+}M_2^{2+}$ is converted to $M_1^{2+}M_2^{3+}$ (Figure 1). The finite electrical resistivity (Figure 9) shows that a real-space distribution of the electrons can be altered by the AC electric field. The motion of the electric dipole in RFe$_2$O$_4$ (R = Y, Ho−Lu) is attributable to the above-described electron transfer, that is, $Fe^{3+}Fe^{2+} \leftrightarrow Fe^{2+}Fe^{3+}$.[1] Indeed, Q was found to be comparable to E for RFe$_2$O$_4$ (R = Er, Yb, and Lu, $Q \sim 0.26-0.30$ eV, $E \sim 0.23-27$ eV).[4,27] The Q and E values of InFe$_2$O$_4$ (Table 2) imply that this mechanism is also true for this material. In addition, the value of T_C of InFe$_2$O$_4$ (Table 2), close to those of RFe$_2$O$_4$, suggests the existence of charge ordering because T_C is affected by a spatial arrangement of Fe^{2+} and Fe^{3+} spins above T_C.

The above-described electron-transfer scenario also explains the dielectric constant of nearly zero at low temperatures (Figure 6); this behavior is ascribed to a suppression of the motion of the polar regions, originating from a reduction of the electron transfer. Therefore, these discussions strongly suggest that electron transfer has an essential role in the dielectric response of the oxides isostructural with RFe$_2$O$_4$, as supported in the next subsection. However, a few issues remain. The conversion between $M_1^{3+}M_2^{2+}$ and $M_1^{2+}M_2^{3+}$ should be confirmed. Thus, resonant XRD measurements on single crystals need to be performed to observe the polar structure.[1] The electron conduction across Cu^{2+} ($3d^9$) and the non-magnetic Ga^{3+} ($3d^{10}$) must be confirmed as well. For this purpose, determining the charge-density distribution may be helpful; this can be done by means of synchrotron XRD combined with the maximum entropy method.[48]

We also make some brief comments on α. The large α values of InFeCuO$_4$ and InGaCuO$_4$ (∼0.3) at around room temperature (Figure 7b) show that the motion of the polar regions is lacking in coherency, which is understandable from the magnetic study of LuFeMgO$_4$.[23] Namely, the Fe-site substitution leads to a distribution of the sizes of the polar regions, and such a distribution lowers the coherent dielectric response. The α decreased as the temperature decreased (Figures 7a and 7b, Table 2), likely indicating that the thermal fluctuation of the dielectric response was suppressed by a decrease in perturbation from phonons. Thus, we can assume that α is a measure of randomness by the thermal effect as well as a measure of either spatial randomness or heterogeneity originating from the Fe-site substitution.

(B) Comparison with the Rare-Earth Systems. The magnetic properties exhibit a relationship with the Yb-, Lu- and In series (Table 2).[27] T_C is decreased with a decrease in the ionic radius of the R ion in RFe$_2$O$_4$: T_C is ∼256 K for YbFe$_2$O$_4$, ∼250 K for LuFe$_2$O$_4$, and ∼242 K for InFe$_2$O$_4$. On the other hand, the tendency is opposite for the Cu-substituted system: T_C is ∼45 K for YbFeCuO$_4$, ∼47 K for LuFeCuO$_4$, and ∼70 K for InFeCuO$_4$. When the R-site ion is changed from Yb to In, the a-length becomes shortened while the c-length is elongated.[27] Thus, the magnetic interaction inside the a-b plane is enhanced, whereas that between the adjacent a-b planes (i.e., upper and lower layers in Figure 1) is weakened. The experimental results mean that the values of T_C for RFe$_2$O$_4$ and RFeCuO$_4$ are mainly governed by the interactions between the a-b plane and inside the a-b plane, respectively.

The ε values of InFeCuO$_4$ (∼6000) and InGaCuO$_4$ (∼1600) at around room temperature (Table 2) are appreciably larger than those of RFeCuO$_4$ (∼100−200) and RGaCuO$_4$ (∼10), which is in agreement with the discussion based on the electron transfer mentioned in subsection **(A)** because the resistivities of InFeCuO$_4$ and InGaCuO$_4$ are lower than those of RFeCuO$_4$ (∼10^8 Ω cm) and RGaCuO$_4$ (>∼10^{8-9} Ω cm), respectively. The higher T_C for InFeCuO$_4$ (Table 2) than that for RFeCuO$_4$ is also interpreted in this context, taking into account the exchange interaction discussed in connection with the electron transfer in subsection **(A)**.

The α values of InFeCuO$_4$ and InGaCuO$_4$ ($\alpha \sim 0.12-0.15$, below 250 K) are smaller than those of RFeCoO$_4$, RFeCuO$_4$, and RGaCuO$_4$ ($\alpha \sim 0.3-0.4$, at around 300 K).[27] That of RFeCoO$_4$ at ∼230−250 K was found to be $\alpha \sim 0.3$. Although α could not be obtained for RFeCuO$_4$ and RGaCuO$_4$ below 250 K because of an ambiguity arising from the small ε (<∼10), InFeCuO$_4$ and InGaCuO$_4$ are homogeneous materials compared to the rare-earth series. This result is in accord with the large ε of InFeCuO$_4$ and InGaCuO$_4$ because a coherent response gives rise to a large dielectric constant.

InFe$_2$O$_4$ exhibits comparable or smaller dielectric constants ($\varepsilon \sim 10000$ for ∼300−1000 Hz) than those of RFe$_2$O$_4$ (R = Yb and Lu, $\varepsilon \sim 10000-20000$ for ∼300−1000 Hz) at around room temperature in spite of the smaller resistivity.[27] The result is consistent with the larger α value of InFe$_2$O$_4$ ($\alpha \sim 0.15$) than that of RFe$_2$O$_4$ (α∼0.1) (Table 2, ref 27), that is, lower coherency in InFe$_2$O$_4$ than in RFe$_2$O$_4$. The difference in coherency is indicative of greater randomness in InFe$_2$O$_4$, which may correlate with the greater oxygen deficiency in InFe$_2$O$_4$ than in RFe$_2$O$_4$ (Experimental Procedures section). Note that ε of ErFe$_2$O$_4$ is different ($\varepsilon \sim 20000-60000$), depending on the oxygen content.[4]

The above discussions combined with those in subsection **(A)** show that although the origins of some experimental results need to be clarified, the overall dielectric properties

(48) See, for example, Takase, K.; Sato, K.; Shoji, O.; Takahashi, Y.; Takano, Y.; Sekizawa, K.; Kuroiwa, Y.; Goto, M. *Appl. Phys. Lett.* **2007**, *90*, 161916.

of the indium oxides strongly support the explanation for the rare-earth systems based on an electron transfer between the Fe-site ions.[27] Therefore, we propose that the dielectric properties of the oxides isostructural with RFe$_2$O$_4$ are plausibly governed by electron transfer; this situation is different from that of ordinary ferroelectrics and dielectrics, in which the displacement of cations and anions plays an essential role. A correlation between the dielectric response and the electron transfer was also suggested for the giant-dielectric-constant material, $CaCu_3Ti_4O_{12}$ (CCTO).[49]

(C) Possible Applications. We have shown that RFeCoO$_4$ may be suitable for applications.[27] This material shows a large ε of $\sim$1000$-$2000 at around room temperature and is prepared by the simple method of firing in air. The resistivity at room temperature is $\sim 10^7$ Ω cm, higher than that of RFe$_2$O$_4$ ($\sim 10^2 \sim 10^3$ Ω cm), and the energy loss is lower than that in RFe$_2$O$_4$. The Q values of $\sim$0.37 eV are comparable to those of RFe$_2$O$_4$ ($Q \sim$ 0.26–0.30 eV),[1,4,5,8,16,27] offering the possibility of the fabrication of fatigue-free devices.[1] A small Q and a large ε have been found for the perovskites La$_2$RuMO$_6$ (M = Ni and Co)[50] and $Tb_{0.5}Ca_{0.5}MnO_3$;[51] an electron transfer may be important in their dielectric responses.

$InFeCuO_4$ and $InGaCuO_4$ are also favorable for application since they show similar properties to those of RFeCoO$_4$; that is, large ε values of $\sim$1000$-$6000 at around room temperature and Q values of $\sim$0.29$-$0.4 eV. Their resistivities are comparable to those of RFeCoO$_4$ (Table 2, ref 27). Furthermore, the materials offer potential energy-saving advantages because the firing temperature of $\sim$1000 °C is lower than that required for RFeCoO$_4$ ($\sim$1380 °C).

As shown in Figure 8, tan δ exhibits peak values (typically, $\sim$2$-$5) at some temperatures for both $InFeCuO_4$ and $InGaCuO_4$. Thus, the dielectric response involves a considerable energy loss. On the other hand, tan δ also takes minimum values of less than 1. For example, the tan δ of $InGaCuO_4$ is $\sim$0.5 at $\sim$280$-$300 K for $< \sim$100 Hz. Accordingly, an operation at $\sim$280$-$300 K is advantageous for $< \sim$100 Hz because of the lowest energy loss with the large ε (Figure 6). This fact reveals the possible application by the selection of the optimum temperature and AC frequency. Thus, our aim is to obtain a further decrease in tan δ (i.e., an increase in resistivity) to reduce energy loss. As stated in subsection **(A)**, the dielectric response is likely rooted in a reversal of the polar regions, arising from the electron transfer between the Fe-site ions. In this context, one possible strategy to increase resistivity without reducing ε is to restrict the electron transfer inside small domains, which may be realized by methods used to generate small particles, such as sputtering and aerosol deposition.[52] In addition, a partial substitution by nonmagnetic ions (such as Mg^{2+}) may be effective to increase resistivity, although ε would be suppressed by a lowering of electron transfer. The results will be presented in the future.

Summary

The magnetic and dielectric properties of $InFe_2O_4$, $InFeCuO_4$, and $InGaCuO_4$ were investigated. All the materials are isostructural with RFe$_2$O$_4$ (R = Y, Ho$-$Lu), which shows ferroelectricity due to iron-valence ordering. $InFe_2O_4$ exhibits ferrimagnetic ordering at $T_C \sim$ 242 K and a dielectric constant (ε) of $\sim$10000 at around room temperature. These properties are similar to those of RFe$_2$O$_4$; the origins of the magnetic and dielectric phenomena are likely common in $InFe_2O_4$ and RFe$_2$O$_4$. From the measurements of the other two materials, we found that both T_C and ε are decreased in the order of $InFe_2O_4$, $InFeCuO_4$, and $InGaCuO_4$. This result strongly supports the explanation based on an electron transfer between the Fe-site ions, as previously discussed for the corresponding rare-earth systems. Therefore, we propose that the dielectric properties of the oxides isostructural with RFe$_2$O$_4$ are plausibly governed by an electron transfer; this situation is different from that of ordinary ferroelectrics and dielectrics, in which the displacement of cations and anions is important. In addition, $InFeCuO_4$ and $InGaCuO_4$ exhibit large ε values ($\varepsilon > \sim$ 1500). In consideration of this property, we discussed the possible applications for these oxides.

Acknowledgment. This work was partially supported by a Grant-in-Aid for Scientific Research (C) from the Ministry of Education, Culture, Sports, Science and Technology.

IC702365K

(49) Wang, C. C.; Zhang, L. W. *Appl. Phys. Lett.* **2007**, *90*, 142905.
(50) Yoshii, K.; Ikeda, N.; Mizumaki, M. *Phys. Status Solidi* **2006**, *A203*, 2812.
(51) Hiramitsu, Y.; Yoshii, K.; Yoneda, Y.; Mizuki, J.; Nakamura, A.; Shimojo, Y.; Ishii, Y.; Morii, Y.; Ikeda, N. *Jpn. J. Appl. Phys.* **2007**, *46*, 7171.
(52) Akedo, J.; Lebedev, M. *Jpn. J. Appl. Phys.* **1999**, *38* (9B), 5397.